Synthesis of Novel Side-Chain Triphenylamine Polymers with Azobenzene Moieties via RAFT Polymerization and Investigation on Their Photoelectric Properties

Yan Sun, Nianchen Zhou, Wei Zhang, Yaowen Li, Zhenping Cheng, Jian Zhu, Zhengbiao Zhang, Xiulin Zhu

Jiangsu Key Laboratory of Advanced Functional Polymer Design and Application, College of Chemistry, Chemical Engineering and Materials Science, Soochow University, Suzhou 215123, China
Correspondence to: N. Zhou (E-mail: nczhou@suda.edu.cn) or X. Zhu (E-mail: xlzhu@suda.edu.cn)

Received 15 March 2012; accepted 29 April 2012; published online
DOI: 10.1002/pola.26167

ABSTRACT: Two novel and well-defined polymers, poly[6-(5-(diphenylamino)-2-((4-methoxyphenyl)diazenyl)phenoxy)hexyl methacrylate] (PDMMA) and poly[6-(4-((3-ethynylphenyl)diazenyl) phenoxy)hexyl methacrylate] (PDPMMA), which bear triphenylamine (TPA) incorporated to azobenzene either directly (PDMMA) or with an interval (PDPMMA) as pendant groups were successfully prepared via reversible addition-fragmentation chain transfer polymerization technique. The electrochemical behaviors of PDPMMA and PDMMA were investigated by cyclic voltammograms (CV) measurement. The hole mobilities of the polymer films were determined by fitting the *J*-V (current-voltage) curve into the space-charge-limited current method. The influence of photoisomerization of the azobenzene moiety on the behaviors of fluorescence emission, CV and hole mobilities of these two polymers were studied. The fluorescent emission intensities of these two polymers in CH_2Cl_2 were increased by about 100 times after UV irradiation. The oxidation peak currents (I_{OX}) of the PDMMA and PDPMMA in CH_2Cl_2 were increased after UV irradiation. The photoisomerization of the azobenzene moiety in PDMMA had significant effect on the electrochemical behavior, compared with that in PDPMMA. The changes of the hole mobility before and after UV irradiation were very small for both polymers. The HOMO energies (E_{HOMO}, HOMO: the highest occupied molecular orbital) of side chain moieties of TPA incorporated with *cis*-isomer and *trans*-isomer of azobenzene in PDMMA and PDPMMA were obtained by theoretical calculation, which are basically consistent with the experimental results. © 2012 Wiley Periodicals, Inc. J Polym Sci Part A: Polym Chem 000: 000–000, 2012

KEYWORDS: azobenzene; fluorescence; hole mobility; living polymerization; reversible addition fragmentation thermal properties chain transfer (RAFT); triphenylamine

INTRODUCTION Triphenylamine (TPA)-based compounds were widely used as materials of photoconducter, organic light-emitting diode, organic solar cell, and so on,[1–4] because TPA is an unique molecule possessing multiple properties, such as redox, fluorescence, particularly good hole-transport. The versatility of TPA compounds has attracted much attention in the field of polymer science. Over the past decade, TPA-containing polymers with the fine photoelectric performance have been successively reported, and various attempts were made to improve the photoelectric properties of these polymers.[5–9] Kolb et al. firstly reported the hole injecting polymer for an electroluminescent element by radical polymerization of a TPA-containing methacrylate monomer.[6] Zentel et al. prepared the block copolymers with TPA and dopamine anchor as side-chain groups via reversible addition-fragmentation chain transfer (RAFT) polymerization, which were bounded to oxidic semiconductors like TiO_2, SnO_2, and ZnO.[7] Peter and Thelakkat synthesized bifunctional polymers carrying tris(bipyridyl)ruthenium(II) and TPA units as pendant groups via atom transfer radical polymerization method.[8]

Azobenzene chromophore has unique reversible photoisomerization property between the *trans*-to-*cis* isomers, where large changes occur in its size, shape, and polarity.[10,11] In recent years, the studies on the versatility of azobenzene derivatives as promising systems for various applications have been developed.[12–14] Most of these studies were focused on the properties of the multi-functional compounds modulated by the azobenzene photoisomerization. Aida and coworkers succeeded in designing "light-driven molecular scissors" by incorporating azobenzene with ferrocene unit.[12] The scissors-like open-close motion was induced by photoisomerization of the azobenzene unit, due to the pivotal motion of the connecting ferrocene unit. Sakai et al. reported a drastic viscosity change of the azobenzene-modified cationic surfactant under the *trans-cis* photoisomerization.[13] Zhu

Additional Supporting Information may be found in the online version of this article.

and coworkers studied the influence of azobenzene photoisomerization on the electronic property of the azobenzene-functionalized tetrathiafulvalene (TTF).[15] The reversible modulation of the electron-donating ability of the TTF moiety was achieved by UV and visible light irradiation, respectively. A few studies on the polymers carrying TPA and azobenzene group have also been reported.[16,17] Fukuzumi and coworkers synthesized poly[9,9-bis(4-diphenylaminophenyl)-2,7-fluorene] which can act as an electroactive component with long-lived charge-separated states, by functionalizing with two moieties of 4-nitroazobenzene at both ends of the polymer chain as withdrawing groups.[16] Choi and coworkers et al. synthesized four different polyoxetanes bearing 4-(*N,N*-diphenyl) amino-4′-azobenzene chromophores in the side chain with short or long spacers to the main chain, and studied the reversible polarization gratings on thin films of those polymers.[17] So far, the investigation on the influence of the azobenzene photoisomerization on the properties of polymers containing azobenzene and TPA groups was rarely reported. TPA unit has the good electrochemical behaviors and hole-mobility due to the easy oxidizability of the nitrogen center. The photoelectric properties of the TPA moiety can be affected by the photoisomerization of azobenzene incorporated to TPA group. It is possible to modulate the oxidizability of the nitrogen center of TPA by means of the change of size, shape, and polarity of *trans*- or *cis*- azobenzene under UV/visible light irradiation. Herein, we designed and prepared two dual functional methacrylate monomers carrying TPA and azobenzene groups, 6-(5-(diphenylamino)-2-((4-methoxyphenyl)diazenyl)phenoxy) hexyl methacrylate (DMMA) and 6-(4-((3-ethynylphenyl)diazenyl)phenoxy)hexyl methacrylate (DPMMA), and prepared their corresponding polymers, poly[6-(5-(diphenylamino)-2-((4-methoxyphenyl)-diazenyl)phenoxy)hexyl methacrylate] (PDMMA) and poly[6-(4-((3-ethynylphenyl)diazenyl)phenoxy)hexyl methacrylate] (PDPMMA), via RAFT polymerization. The effect of photoisomerization of azobenzene unit on the fluorescence emission, electrochemical behaviors and the hole mobility of these two polymers were investigated.

EXPERIMENTAL SECTION

Materials

All chemicals were purchased from Shanghai Chemical Reagent Co., Shanghai, China and used as received unless otherwise stated. Tetrahydrofuran (THF), toluene and methylene chloride were dried and distilled with standard methods before use. 2,2′-Azobis(isobutyronitrile) (AIBN, ≥98%) were recrystallized twice from ethanol before use. Tetrabutylammonium fluoride (99%, J&K Chemical) was recrystallized from ethyl acetate. Copper (I) bromide (CuBr, 98%) was washed with acetic acid and acetone, and then dried in vacuum. 3-Ethynylaniline (≥98%, Aldrich), sodium azide (99.5%, Aldrich), sodium *ter*-butoxide (≥98%; Acros), palladium (II) acetate (J&K Chemical, 99%), diphenylamine, 3-bromophenol, and tri-*t*-butylphosphine (J&K Chemical, ≥99%, 10 wt % in hexane) were used as received. 2-Cyanoprop-2-yl-1-dithionaphthalate (CPDN, 97%) was synthesized according to the method as reported.[18]

Synthesis

3-(Diphenylamino)phenol (compound (1)) and 4-(diphenylamino)phenol (compound (2))

The synthetic procedures of compounds (1) and (2) are presented in Scheme 1.[19] The typical synthetic procedure of compound (1) is as follows: A solution of 3-bromophenol (8.6 g, 49 mmol), diphenylamine (8.45 g, 50 mmol), sodium *ter*-butoxide (12.5 g, 130 mmol), tri-*t*-butylphosphine (0.5 g, 2.5 mmol) and palladium acetate (0.0050 g, 0.0074 mmol) were mixed in 100-mL dry toluene in a 250-mL round bottom flask under vigorous stirring. The resulted mixture was refluxed for 30 min, and then was allowed to room temperature. Then ethyl acetate (100 mL) was added. The mixture was washed with deionized water (3 × 100 mL). After being dried over anhydrous $MgSO_4$ overnight, ethyl acetate was evaporated under reduced pressure. The remaining mixture was poured into 100-mL petroleum ether under stirring. After filtration compound (1) was obtained as white solid (10.2 g, yield 80.0%). ^{1}H NMR (300 MHz, DMSO-d_6), δ(tetramethylsilane, TMS, ppm): 9.34 (s, —O*H*), 7.29 (t, 4H, Ar*H*), 7.13–6.90 (m, 7H, Ar*H*), 6.47-6.37 (m, 3H, Ar*H*). The yield of compound (2) is 75.5%. ^{1}H NMR (300 MHz, DMSO-d_6), δ (TMS, ppm): 9.42 (s, —O*H*), 7.42–7.17 (m, 4H, Ar*H*), 6.91 (t, 8H, Ar*H*), 6.75 (d, 2H, Ar*H*).

6-(5-(Diphenylamino)-2-((4-methoxyphenyl)diazenyl) phenoxy)hexyl methacrylate (DMMA (3)) and 6-(4-((3-ethynylphenyl)diazenyl)phenoxy)hexyl methacrylate (compound (4))

DMMA and compound (4) were prepared through diazotization, reactions of azo-coupling, etherification, and acylation procedures according to the method reported in the literature.[20] ^{1}H NMR of DMMA (300 MHz, $CDCl_3$), δ (TMS, ppm): 7.57 (d, 1H, Ar*H*), 7.35–7.15 (m, 7H, Ar*H*), 7.10 (d, 2H, Ar*H*), 6.92 (s, 3H, Ar*H*), 6.86–6.65 (m, 4H, Ar*H*), 6.09 (s, 1H, C=CH_2), 5.54 (s, 1H, C=CH_2), 4.15 (s, 2H, —CH_2—), 3.91 (s, 2H, —CH_2—), 3.80 (s, 3H, —OCH_3), 1.93 (s, 3H, —CH_3), 1.70 (s, 4H, —CH_2CH_2—), 1.25 (s, 4H, —CH_2CH_2—). ^{1}H NMR of compound (4) (300 MHz, DMSO-d_6), δ (TMS, ppm): 7.98–7.83 (m, 4H, Ar*H*), 7.60 (m, 2H, Ar*H*), 7.13 (d, 2H, Ar*H*), 6.01 (s, 1H, C=CH_2), 5.66 (s, 1H, C=CH_2), 4.34 (s, 1H, ArC≡*H*), 4.09–4.15 (m, 4H, —OCH_2—), 1.87 (s, 3H, —CH_3), 1.80–1.70 (m, 2H, —CH_2—), 1.70–1.58 (m, 2H, —CH_2—), 1.42 (m, 4H, —CH_2—).

4-(Diphenylamino)phenyl 6-azidohexanoate (compound (5))

Compound (5) was synthesized through the acylation reaction of compound (2) with 6-bromohexanoyl chloride and then azide reaction. Detailed synthetic procedures were similar with those as reported.[20] FTIR (KBr): γ_{max}/cm^{-1} 2930, 2860, 2100, 1760, 1600, 1500, 1460, 750, and 700.

(4-(Diphenylamino)phenyl-6-(4-(3-((4-((6-(methacryloyloxy)hexyl)oxy)phenyl) diazenyl)phenyl)-1,2,3-triazol-1-yl)hexanoate) (DPMMA)

The mixture of compound (4) (2.2 g, 5.5 mmol), compound (5) (2.0 g, 5.0 mmol), CuBr (0.0025 g, 0.500 mmol) and *N,N,N′,N″,N‴*-pentamethyldiethylenetriamine (PMDETA,

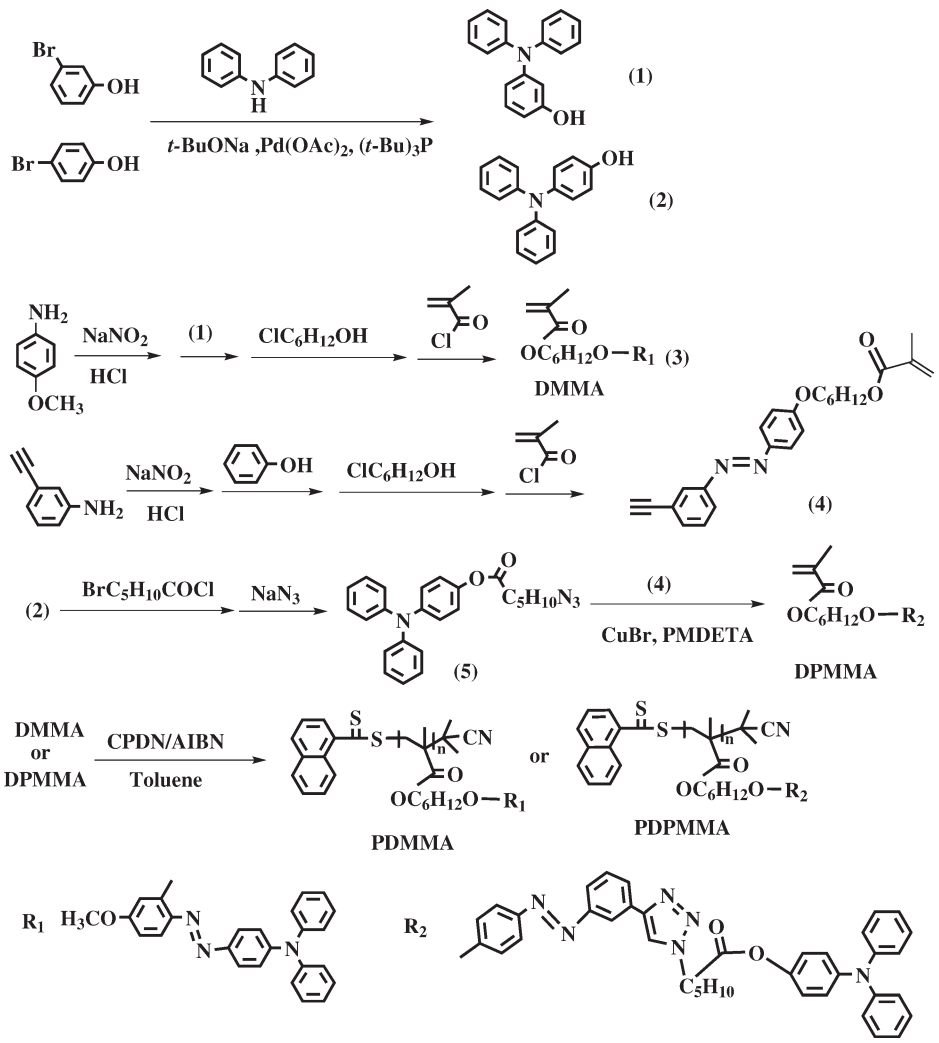

SCHEME 1 The synthetic routes of DMMA, DPMMA, PDMMA and PDPMMA.

105 μL, 0.500 mmol) were dissolved in 10 mL THF in a 25-mL single-necked flask. The reaction mixture was vigorously stirred in deoxygenated system at room temperature for 24 h. After that, the content was evaporated in a reduced pressure and purified by column chromatography (silica gel, ethyl acetate/petroleum ether = 1:8) to yield a yellow solid (7.9 g, 90%). ^{1}H NMR (300 MHz, $CDCl_3$), δ(TMS, ppm): 8.15 (s, 1H, —C_2HN_3—), 8.08–7.85 (m, 4H, Ar*H*), 7.25 (d, 8H, Ar*H*), 7.22—6.91 (m, 10H, Ar*H*), 6.11 (s, 1H, C=CH_2), 5.56 (s, 1H, C=CH_2), 4.18 (t, 2H, —CH_2—), 4.06 (t, 2H, —CH_2—), 1.95 (s, 3H, —CH_3), 1.85 (t, 2H), 1.73 (t, 2H, —CH_2—), 1.54 (d, 6H, —CH_2—), 1.21 (s, 8H, —CH_2—).

RAFT Polymerization

The typical procedure of RAFT polymerization is as follows: DMMA (0.5 g, 0.8900 mmol), AIBN (1.46 mg, 0.0089 mmol), and CPDN (8.13 mg, 0.0267 mmol) were dissolved in 1.5 mL of toluene in a 5-mL ampoule tube. After purging with argon for about 10 min to eliminate the oxygen, the ampoule tube was sealed and placed in an oil bath held by a thermostat at 75 °C to polymerize. After designed time interval, the tube was cooled in ice water and then opened. The contents were dissolved in 2 mL of THF, and then poured into 400 mL of methanol. The polymer (PDMMA) was obtained by filtration and then dried in vacuum overnight at 40 °C. The monomer conversion is 74.0% as determined gravimetrically. The RAFT polymerization procedure of DPMMA is similar with those described above. The monomer conversion is 63.0%.

Characterization

^{1}H NMR spectra were recorded on a Inova 300-MHz NMR instrument, using deuterated chloroform ($CDCl_3$) or deuterated dimethyl sulfoxide (DMSO-d_6) as the solvent, TMS as the internal standard. The number-average molecular weight ($M_{n,GPC}$) and polydispersity index value (PDI = M_w/M_n) of the polymers were determined with a Waters 1515 gel permeation chromatograph (GPC) equipped with a refractive index detector, HR1(pore size: 100 Å, 100–5000 Da), HR2(pore size: 500 Å, 500–20, 000 Da), and HR4 (pore size 10, 000 Å, 50–100, 000 Da) columns (7.8 × 300 mm, 5-μm beads size) with a molecular weight range of 100–500 000 and calibrated with poly(methyl methacrylate) (PMMA) as the standard sample. Tetrahydrofuran (THF) was used as the eluent at a flow rate of 1.0 mL/min at 30 °C. FTIR spectra

TABLE 1 Macromolecular Characteristics and Photoisomerization Data of Polymers (PDMMA and PDPMMA)

Entry	$[Monomer]_0/[AIBN]_0/[CPDN]_0$	$M_{n,th}$ (g/mol)	$M_{n,GPC}$ (g/mol)	M_w/M_n	k_e s^{-1}	*cis*/*trans*
PDMMA	100/1/3	14200	13600	1.16	0.014	1.92
PDPMMA	100/1/3	16900	18000	1.18	0.010	0.73

$M_{n,th}$ is the theoretical molecular weight.
$M_{n,GPC}$ is the number average molecular weight measures by GPC using PMMA as the standard.
M_w/M_n is molecular weight distribution measured by GPC. k_e is the first-order rate constant.
The *cis*/*trans* is the *cis*/*trans* ratio of azobenzene in the photostationary state on the basis of the π-π^* absorbance.

were recorded on a Nicolette-6700 FTIR spectrometer. Ultraviolet visible (UV-*vis*) absorption spectra were determined on a Hitachi U-3900 spectrophotometer at room temperature. The fluorescence emission spectra of the polymers were obtained on a PerkinElmer LS-50B fluorescence spectrophotometer at room temperature. The spherical aggregate size analysis was performed using dynamic light scattering (DLS) measurements (Zetasizer Nano ZS: Malvern Instrument, UK) at 20 °C. The micellar solutions were filtered through a 0.45-μm syringe filter before measurements. Cyclic voltammograms (CV) were carried out with an electrochemical analyzer (CHI630B, Shanghai Chenghua instrument Co. China) using $C_{16}H_{36}F_6NP$ (tetrabutylammonium hexafluorophosphat) (0.1 M) as the supporting electrolyte and calomel electrode as reference electrode at a scan rate of 0.1 V/s in CH_2Cl_2. The measurement was conducted at room temperature under an oxygen-free atmosphere.

Fabrication and Characterization of Devices for Hole Mobility

For device fabrication, indium tin oxide (ITO) coated glass substrates were cleaned stepwise in semiconductor detergent, deionized water, chloroform, acetone, and isopropanol and then dried in a 110 °C oven for 20 min, subsequently, the substrates were treated with UV ozone for 5 min before use. A thin layer (ca. 39 nm) of poly(ethylenedioxythiophene): polystyrenesulfonate (PEDOT: PSS, Baytron P VP AI 4083) was spin-coated (3500 rpm) onto the ITO substrates. After baking at 125 °C for 20 min in air, the substrates were transferred to a N_2-filled glovebox. The active layers (~90 nm) were spin-coated on the PEDOT: PSS layer from the polymer solution in chloroform with weight concentration of 15 mg/mL before or after UV irradiation, respectively. The devices were ready for measurement after thermal deposition of a 40 nm-thick film of Au at a pressure of 1×10^{-6} mbar. The effective layer area of one cell was 0.12 cm^2. For mobility measurements, the hole-only devices in a configuration of ITO/PEDOT: PSS (39 nm)/polymer/Au (40 nm) were fabricated. The current density-voltage (*J*-V) characteristics were measured using a Keithley 2400 source meter. All measurements were performed under ambient atmosphere at room temperature. The hole mobility was determined by fitting *J*-V curve into the space-charge-limited current (SCLC) method[21] based on the formula (1).

$$J = \frac{9}{8}\varepsilon_r\varepsilon_0\mu_h\frac{V^2}{L^3} \quad (1)$$

where ε_0 is the permittivity of free space, ε_r is the dielectric constant of the material, μ_h is the hole mobility, V is the voltage drop across the device, and L is the thickness of active layer.

RESULTS AND DISCUSSION

Preparation of PDMMA and PDPMMA via RAFT Polymerizations

The synthetic routes of the polymers, PDMMA and PDPMMA, are presented in Scheme 1. PDMMA and PDPMMA were synthesized via RAFT polymerization of DMMA and DPMMA in toluene at 75 °C using CPDN as the RAFT agent and AIBN as the initiator. The polymerization data of DMMA and DPMMA were given in Table 1. It can be noted that the molecular weights measured by GPC ($M_{n,GPC}$) of these two polymers were very close to the corresponding theoretical values ($M_{n,th}$). The GPC elution curves of PDMMA and PDPMMA given in Figure 1 exhibited narrow and symmetric shapes with relatively narrow molecular weight distributions (M_w/M_n). Furthermore, the structures of PDMMA and PDPMMA were also characterized by ^1H NMR spectra as shown in Figure 2(A,B). The chemical shifts at δ = 8.14–8.06 ppm (a) were attributed to the protons of the naphthaline groups (a) in the end of polymer chains, which indicated that the RAFT agent species were sucessfully attached to the chain ends of PDMMA and PDPMMA, respectively. These results confirmed

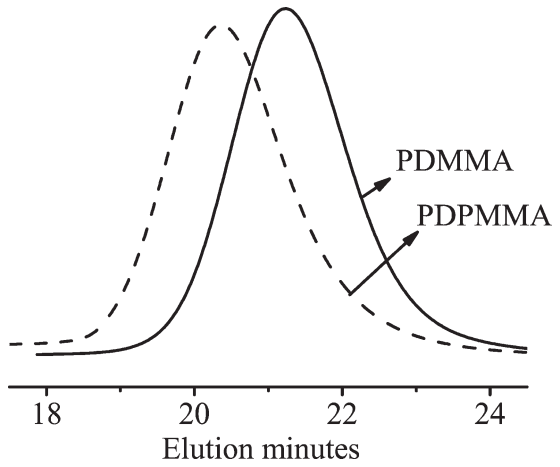

FIGURE 1 GPC curves of PDMMA ($M_{n,GPC}$ = 13600 g/mol, M_w/M_n = 1.16) and PDPMMA ($M_{n,GPC}$ = 18000 g/mol, M_w/M_n = 1.18).

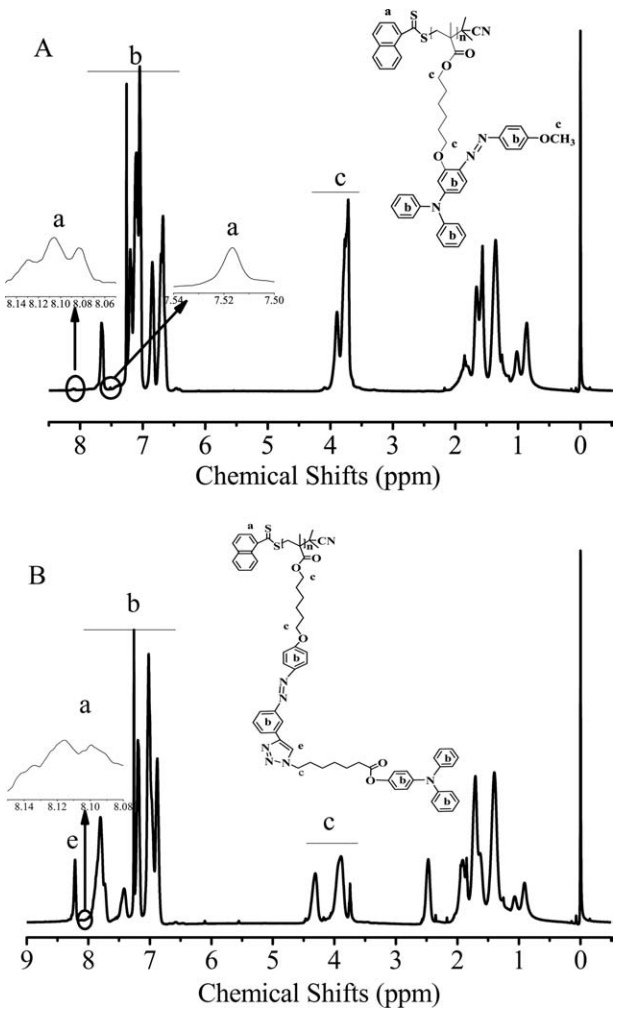

FIGURE 2 Typical ^{1}H NMR specta of PDMMA (A, solvent $CDCl_3$, $M_{n,GPC}$ = 13600 g/mol, M_w/M_n = 1.16) and PDPMMA (B, solvent $CDCl_3$, $M_{n,GPC}$ = 18000 g/mol, M_w/M_n = 1.18) prepared via RAFT polymerization using CPDN as RAFT agent and AIBN as the initiator.

that the well-controlled PDMMA and PDPMMA were successfully prepared by RAFT polymerization.

Photoisomerization

PDMMA and PDPMMA exhibited good solubility in several organic solvents, such as $CHCl_3$, CH_2Cl_2, THF, and so on. The UV-*vis* absorbance spectra of PDMMA and PDPMMA in CH_2Cl_2 were examined, as shown in Figure 3(a,b), respectively. The strong peak at 302 nm corresponds to the TPA unit.[22] Two absorption peaks (centered at 359 and 402 nm) in Figure 3(a) were attributed to the transition bands of π-π* and n-π* related to the groups of *trans*-azobenzene and *cis*-azobenzene in PDMMA, while two absorption peaks (centered at 348 nm and 448 nm) in Figure 3(b) were attributed to the transition bands of π-π* and n-π* related to the groups of *trans*-azobenzene and *cis*-azobenzene in PDPMMA. Upon 365 nm UV light irradiation (0.4 mW/cm^2), the absorption intensity of π-π* transition bands corresponding to *trans*-azobenzene groups significantly decreased, and both the absorption intensity of n-π* transition band corresponding to *cis*-azobenzene gradually increased. The solutions of PDMMA and PDPMMA reached the *cis*-rich stationary states after 365 nm UV light irradiation for 5 and 8 min, respectively. The *cis*/*trans* ratio in the photostationary state was estimated from Figure 3(a,b) with the formula $(A_0\text{-}A_\infty)/A_\infty$, where A_∞ and A_0 are the π-π* absorbance of PDMMA and PDPMMA at time infinite and time zero. The *cis*/*trans* ratio of PDMMA and PDPMMA was 1.92 and 0.73, respectively. The lower *cis*/*trans* ratio of PDPMMA may be ascribed a higher *trans*-to-*cis* transition resistance existed in PDPMMA with more flexible spacers.[23] The kinetic plots of *trans*-to-*cis* photoisomerization of PDMMA and PDPMMA were plotted in Figure 3(c), which indicted the first-order kinetic plots of the PDMMA and PDPMMA. Furthermore, the first-order rate constant (k_e) deduced from Figure 3(c) was determined by formula (2), respectively.

$$\ln\frac{A_\infty - A_t}{A_\infty - A_0} = -k_e t \quad (2)$$

where A_∞, A_0, and A_t are absorbance of π-π* at time infinite, time zero, and time t, respectively. The *trans*-to-*cis* photoisomerization rate constant (k_e) of PDMMA and PDPMMA was 0.014 and 0.010 s^{-1}, respectively. The rate constant of PDPMMA was lower than that of PDMMA. It may be interpreted as the higher degree of inter-chain entanglements existed in PDPMMA with more flexible spacers resulting in a higher *trans*-to-*cis* transition resistance compared with that of PDMMA.[23]

Fluorescence Emission

Some researchers reported that the azobenzene-containing polymers showed the light-driven or aggregation-induced fluorescence emission enhancement.[24–26] In this system, when PDMMA and PDPMMA solutions were excited by 395 nm light corresponded to the n-π* transition band of azobenzene group in PDMMA, almost no fluorescence emission was observed (Figure 4). However, as PDMMA and PDPMMA solutions were exposed to UV light of 365 nm (0.4 mW/cm^2), the fluorescence emission of PDMMA (centered at 560 nm) and PDPMMA (centered at 506 nm) continually increased with irradiation time, respectively. The PDMMA and PDPMMA solutions before and after UV light irradiation were examined by DLS to clarify the cause of the fluorescence enhancement. The results shown in Figure 5 indicated that nano-scale aggregations were formed after irradiation with 365 nm light. The aggregation size was 63 nm for PDMMA and 92 nm for PDPMMA when reaching the photoisomerization equilibrium state. And the aggregation size reached 79 and 113 nm for PDMMA and PDPMMA solution, when prolonging the UV light irradiation time to 10 and 16 min, respectively. Normally, the azobenzene compound is nonfluoresent due to the fast nonradiative relaxation process originated from fast and high efficient *tans*-to-*cis* isomerization for excited azobenzene.[26] However, the aggregation will hinder the excited azobenzene relaxation in a nonradiative way, which resulted in the fluorescence emission.[27] The

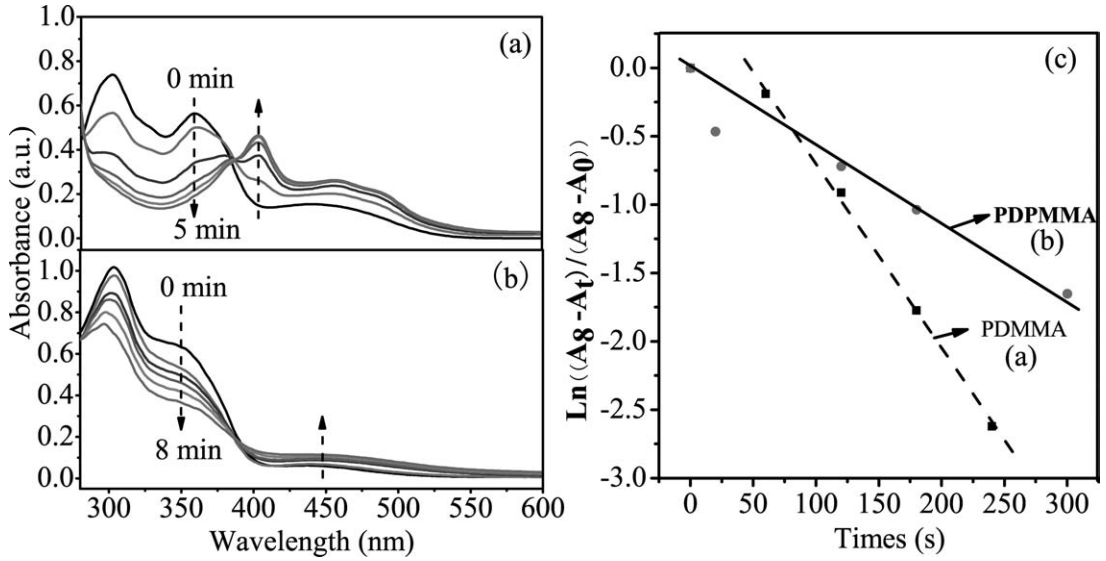

FIGURE 3 UV-*vis* spectra of PDMMA (a) and PDPMMA (b) in CH_2Cl_2 ($C_n = 3 \times 10^{-5}$ mol/L azo mesogens) at ambient temperature as a function of 365 nm light irradiation with different time. (c) Kinetic plots of the *trans*-to-*cis* photoisomerization of azobenzene upon UV irradiation for PDMMA and PDPMMA.

aggregates formation of the azobenzene-containing polymers after UV irradiation should be attributed to the increasing polarity induced by isomerization of azobenzene from its planar rod-shaped *trans*-form to the nonplanar bent-shaped *cis*-form, which resulted in a poor solubility of polymers in non-polar CH_2Cl_2.[28]

Furthermore, bathochromic shift can be seen from the maximum emission peaks of PDMMA (centered at 560 nm) and PDPMMA (centered at 506 nm) in Figure 4. The cause of it may be that the azobenzene group conjugates with the lone electron pair of nitrogen in TPA moiety in case of PDMMA, which leads to the increase of the conjugated length and hence red-shift of the maximum fluorescence emission peak.

Electrochemical Behavior

CV was used to investigate the electrochemical behavior of polymer solutions before and after UV irradiation. Previous studies demonstrated that the azobenzene moiety possesses electrochemical activity.[29] Fujishima and coworkers[29] reported that the reduction potential of gold electrode modified with azobenzene functionalized SAMs was lower than −0.6 V. When the scanning potential was much higher than the reduction potential of azobenzene, it can avoid the electrochemical reduction from azobenzene to hydroazobenzene.[30] Thus, the positive scanning potential was employed in our present work to avoid the reduction of azobenzene group in polymer. Figure 6(a,b) showed the CV curves of

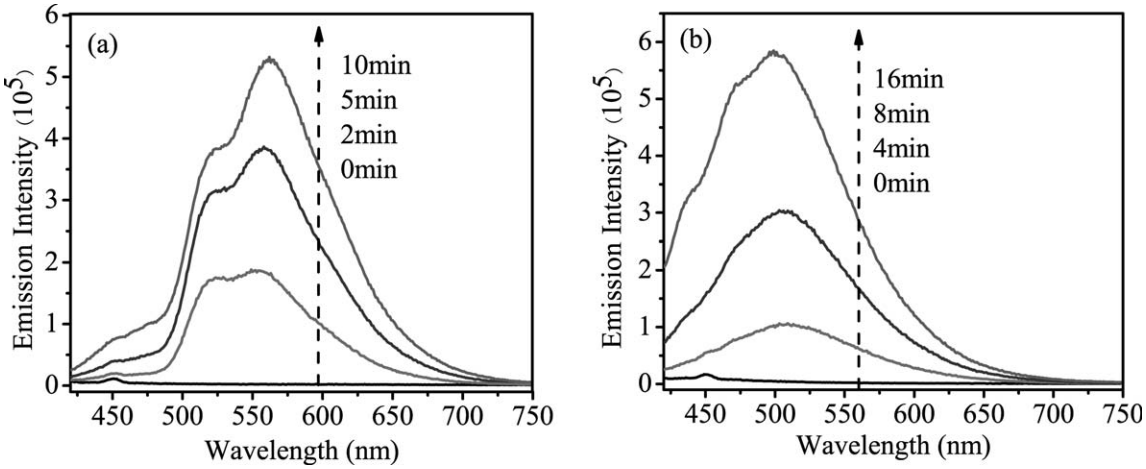

FIGURE 4 Fluorescence emission spectra of PDMMA (a) ($M_{n,GPC} = 13600$ g/mol, $M_w/M_n = 1.16$) and PDPMMA (b) ($M_{n,GPC} = 18000$ g/mol, $M_w/M_n = 1.18$) in CH_2Cl_2 ($C_n = 3 \times 10^{-5}$ mol/L azo mesogens) at ambient temperature ($\lambda_{ex} = 395$ nm) under 365 nm light irradiation (0.4 mW/cm^2) with different time.

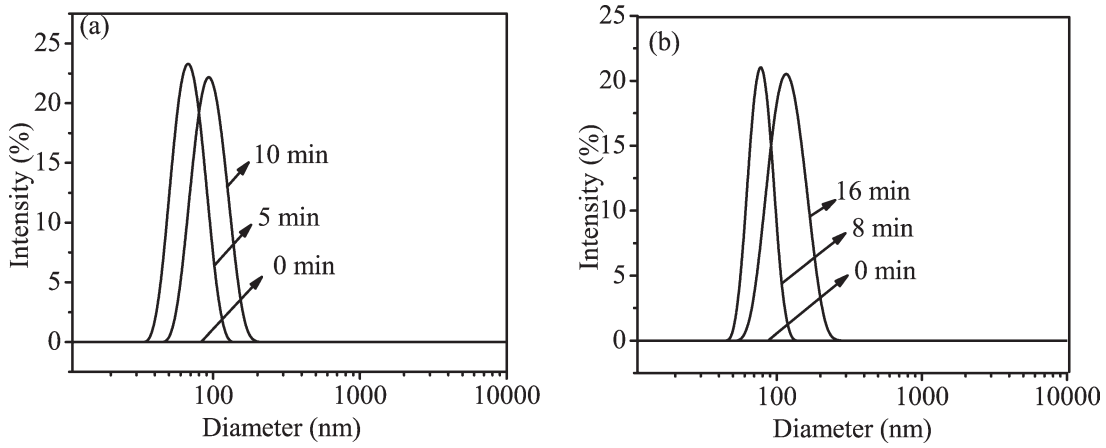

FIGURE 5 DLS curves for the distributions of aggregation sizes of PDMMA (a) and PDPMMA (b).

PDMMA and PDPMMA in CH_2Cl_2 before and after UV irradiation, respectively, and the corresponding data were summarized in Table 2. For better comparison, the solutions used for testing the CV before and after UV irradiation were also analyzed by the UV-*vis* absorption spectra as given in Supporting Information Figure S1. The both peak currents at 0.8–1.0V attributing to the TPA in PDMMA and PDPMMA increased after UV irradiation, which may be caused by the increased concentration of TPA unit around the Pt electrode due to the aggregation in solution after UV irradiation. The difference between the CV curves of PDMMA and PDPMMA was observed from Figure 6. The reversible redox activity of PDPMMA was better than that of PDMMA. For PDMMA, the absence of corresponding reduction peak at 0.8–1.0V indicated poor activities of reversible reduction. The oxidation peak potential (E_{ox}) of PDMMA solution decreased from 0.97 to 0.87 V after UV light irradiation for 12 min, which could indicate the reduction ability (that is, the electron-donating ability) of TPA in PDMMA was increased after UV irradiation. For PDMMA, the TPA can be well conjugated with *trans*-azobenzene group by adopting a planar structure before UV irradiation, as a result, the lone electron pair of the nitrogen atom of TPA was scattered to conjugated system. When the *trans*-form of azobenzene groups translated to *cis*-form in PDMMA after UV irradiation, the conjugation between TPA and azobenzene was greatly weaken because the phenyl rings of *cis*-form twisted around the plane of the nitrogen–nitrogen double bond.[31,32] That is, *cis*-form isomer could prevent the electron density of the nitrogen atom of TPA scattere as compared with that of *trans*-form, causing the increase of electron-donating ability of TPA in PDMMA after UV irradiation. In addition, a new pair of redox peaks at 0.2-0.4V after UV irradiation [Fig. 6(a)] may be belonged to the structures of quinone/hydroquinone derived from TPA unit incorporated directly with azobenzene. The detailed reasons need further study. The redox peak potentials (E_{ox} and E_{red}) of TPA in PDPMMA had a little difference before and after UV irradiation as shown in Figure 6(b), which may be attribute to the weak effect of photoisomerization of the azobenzene on the TPA in PDPMMA, where the TPA moiety was separated from the azobenzene moiety by a flexible spacer.

To verify the electrochemical behavior of the TPA moieties in the PDMMA and PDPMMA, the molecular orbital distribution

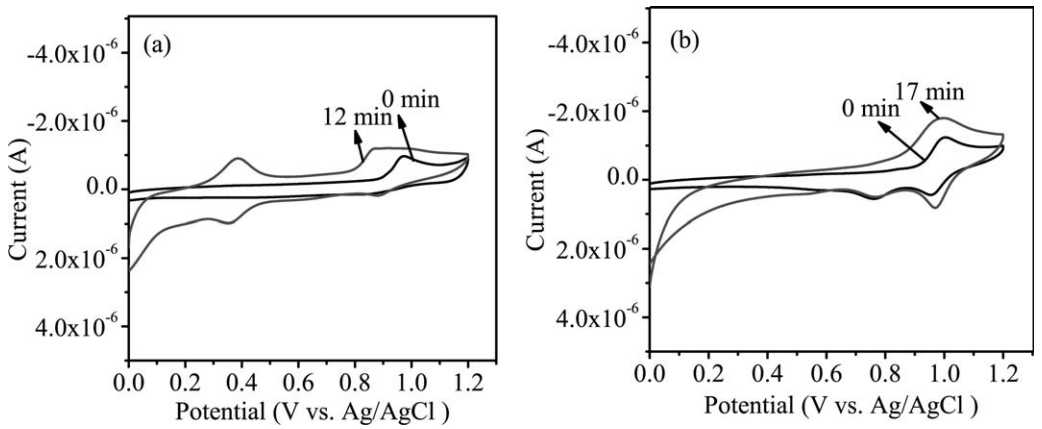

FIGURE 6 Cyclic voltammograms of PDMMA (a) ($M_{n,GPC}$ = 13600 g/mol, M_w/M_n = 1.16) and PDPMMA (b) ($M_{n,GPC}$ = 18000 g/mol, M_w/M_n = 1.18) in CH_2Cl_2 ($C_n = 1 \times 10^{-4}$ mol/L azo mesogens) containing *n*-Bu_4NPF_6 (0.1 M) before and after UV irradiation (0.4 mW/cm^2).

TABLE 2 The Data of Cyclic Voltammograms (CV) and Hole Mobility of Polymers (PDMMA and PDPMMA)

Entry	E_{OX} V	I_{OX} μA	E_{HOMO} (eV)	L^b (nm)	Hole mobility[c] ($cm^2\ V^{-1}\ S^{-1}$)
PDMMA	0.97	−0.96	−4.915	89.5	4.83×10^{-6}[d]
PDMMA-UV[a]	0.87	−1.19	−4.905	83.0	2.87×10^{-6}[e]
PDPMMA	1.00	−1.23	−5.003	96.5	3.66×10^{-6}[d]
PDPMMA-UV[a]	1.00	−1.80	−5.006	83.0	3.18×10^{-6}[e]

[a] The polymer solution are under UV irradiation (0.4 mW/cm^2).
[b] Thickness of the polymer film.
[c] Hole mobility of these polymers in the BHJ blends was calculated via the SCLC method.
[d] Spin coated from a 15 mg/mL chloroform solution.
[e] Spin coated from a 15 mg/mL chloroform solution with UV irradiation to sufficiently reach a *cis*-rich stationary state.

calculations of the side-chain in the PDMMA and PDPMMA were carried out by using quantum mechanical package Gaussian 03, respectively. The optimum geometry and HOMO energies (E_{HOMO}) (HOMO: the highest occupied molecular orbital) of the TPA moiety incorporated with *cis*-isomer or *trans*-isomer of azobenzene in the PDMMA and PDPMMA are calculated by using the density functional theory (DFT) as approximated by the B3LYP functional and employing the 6-31G* basis set[33] as shown in Figure 7 and Table 2. The electron-donating abilities of the TPA moieties in PDMMA and PDPMMA before and after UV irradiation can be represented by their oxidation peak potentials (E_{ox}s), which are related to the corresponding HOMO energy levels (E_{HOMO}s). The both E_{HOMO}s of *cis*- and *trans*-isomers in PDPMMA had a little difference (−5.003 eV for the *trans*-isomer and −5.006 eV for the *cis*-isomer), and the corresponding E_{ox}s after and before UV irradiation were both 0.96 V. The E_{HOMO} (−4.905 eV) of the *cis*-isomer in PDMMA was a little higher than that of the *trans*-isomer (−4.915 eV), and the E_{ox} (0.87 V) after UV irradiation was lower than that (0.97 V) before UV irradiation. The HOMO energy levels obtained by theoretical calculation were basically consistent with corresponding oxidation peak potentials (E_{ox}s) obtained by CV measurement.

Hole Mobility

Hole mobility is a key parameter to evaluate the carrier transporting property of the hole transport material. TPA unit has the good hole-mobility due to the easy oxidizability of the nitrogen center, which can facilitate to transport positive charge via the radical cation species. The current-voltage

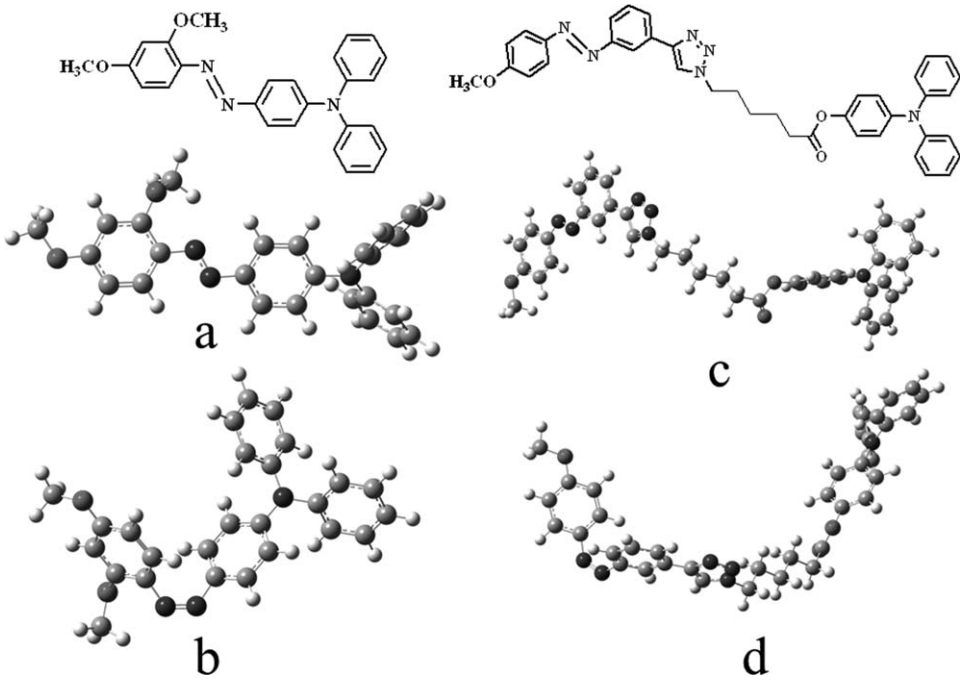

FIGURE 7 Optimized geometries for TPA moieties incorporated with *cis*-isomer and *trans*-isomer of azobenzene in the side-chain of PDMMA and PDPMMA. (a) and (b): *trans*-isomer and *cis*-isomer in the side-chain of PDMMA; (c) and (d) *trans*-isomer and *cis*-isomer in the side-chain of PDPMMA.

(*J*-V) curves of hole devices of the PDMMA and PDPMMA before and after UV irradiation were given in Supporting Information Figure S2. And the corresponding data of the hole mobilities calculated by the SCLC method were presented in Table 2. The testing samples were prepared from the polymer solution ($CHCl_3$) before or after UV irradiation by spin-coating. The hole mobilities before UV irradiation were 4.83 $\times$ 10^{-6} cm^2V^{-1} S^{-1} for PDMMA and 3.66 $\times$ 10^{-6} cm^2V^{-1} S^{-1} for PDPMMA, and these values changed to 2.87 $\times$ 10^{-6} and 3.18 $\times$ 10^{-6} $cm^2V^{-1}S^{-1}$ after UV irradiation, respectively. The hole mobilities of both polymers before and after UV irradiation were very small, which showed the photoisomerization of the azobenzene moieties had no significant effect on the hole mobilities of both polymers. These results may be ascribed to the restraint from the azobenzene moieties on the hole transport of TPA.

CONCLUSION

Two well-defined polymers bearing triphenylamies (TPAs) incorporated to azobenzene units either directly or with an interval as pendant groups, PDMMA and PDPMMA, were successfully prepared via reversible addition-fragmentation chain transfer (RAFT) polymerization technique. The fluorescence emission of these two polymers in CH_2Cl_2 followed by *trans*-to-*cis* photoisomerization significantly increased by about 100 times. The photoisomerization of azobenzene moieties in PDMMA had significant effect on the electrochemical behavior, compared with that in PDPMMA. The difference between hole mobilities of PDMMA and PDPMMA as well as their changes before and after UV irradiation were both very small. The E_{HOMO}s of TPA incorporated with *cis*-isomer and *trans*-isomer of azobenzene in PDMMA and PDPMMA obtained by theoretical calculation were basically consistent with their corresponding oxidation peak potentials (E_{OX}s) obtained by CV measurement. The present studies are expected to provide guideline for the molecular design of TPA-based materials with excellent photoelectric properties, and expand the versatility of TPA-based compounds for the applications in optical materials.

ACKNOWLEDGMENTS

The financial support from the National Natural Science Foundation of China (Nos. 21074082 and 21104052), the Specialized Research Fund for the Doctoral Program of Higher Education contract grant (No.20103201110005), the Project of Science and Technology Development Planning of Suzhou (Nos. SYG201026 and SYG201111), the Project of International Cooperation of the Ministry of Science and Technology of China (No. 2011DFA50530), the Qing Lan Project, the Program of Innovative Research Team of Soochow University, and the Project Funded by the Priority Academic Program Development of Jiangsu Higher Education Institutions (PAPD) are gratefully acknowledged.

REFERENCES AND NOTES

1 Tang, C. W.; Vanslyke, S. A. *Appl. Phys. Lett.* **1987,** *51*, 913–915.

2 Adachi, C.; Nagai, K.; Tamoto, N. *Appl. Phys. Lett.* **1995,** *66*, 2679–2681.

3 Grazulevicius, J. V. *Polym. Adv. Technol.* **2006,** *17*, 694–696.

4 Lu, J. P.; Xia, P. F.; Lo, P. K.; Tao, Y.; Wong, M. S. *Chem. Mater.* **2006,** *18*, 6194–6203.

5 Higashihara, T.; Ueda, M. *Macromolecules* **2009,** *42*, 8794–8800.

6 Kolb, E. S.; Gaudiana, R. A.; Mehta, P. G. *Macromolecules* **1996,** *29*, 2359–2364.

7 Zorn, M.; Zentel, R. *Macromol Rapid Commun.* **2008,** *29*, 922–927.

8 Peter, K.; Thelakkat, M. *Macromolecules* **2003,** *36*, 1779–1785.

9 Behl, M.; Hattemer, E.; Brehmer, M.; Zentel, R. *Macromol. Chem. Phys.* **2002,** *203*, 503–510.

10 Ichimura, K. *Chem. Rev.* **2000,** *100*, 1847–1873.

11 Natansohn, A.; Rochon, P. *Chem. Rev.* **2002,** *102*, 4139–4175.

12 Muraoka, T.; Kinbara, K.; Kobayashi, Y.; Aida, T. *J. Am. Chem. Soc.* **2003,** *125*, 5612–5613.

13 Sakai, H.; Orihara, Y.; Kodashima, H.; Matsumura, A.; Ohkubo, T.; Tsuchiya, K.; Abe, M. *J. Am. Chem. Soc.* **2005,** *127*, 13454–13455.

14 Kondo, T.; Kanai, T.; Uosaki, K. *Langmuir* **2001,** *17*, 6317–6324.

15 Wen, G. Y.; Zhang, D. Q.; Huang, Y. Y.; Zhao, R.; Zhu, L. Y.; Shuai, Z. G.; Zhu, D. B. *J. Org. Chem.* **2007,** *72*, 6247–6250.

16 El-Khouly, M. E.; Chen, Y.; Zhuang, X. D.; Fukuzumi, S. *J. Am. Chem. Soc.* **2009,** *131*, 6370–6371.

17 Cha, S. W.; Choi, D. H.; Oh, D. K.; Han, D. Y.; Lee, C. E.; Jin, J. *Adv. Funct. Mater.* **2002,** *12*, 670–677.

18 Zhu, J.; Zhu, X. L.; Chen, Z. P.; Liu, F.; Lu, J. M. *Polymer* **2002,** *43*, 7037–7042.

19 Yang, B. H.; Buchwald, S. L. *J. Org. Chem.* **1999,** *576*, 125–146.

20 Xue, X. Q.; Zhu, J.; Zhang, Z. B.; Zhou, N. C.; Tu, Y. F.; Zhu, X. L. *Macromolecules* **2010,** *43*, 2704–2712.

21 Blom, P. W. M.; Jong, M. J. M.; Munster, M. G. *Phys. Rev. B* **1997,** *55*, 656–659.

22 Liu, J.; Pei, Q. B.; *Macromolecules* **2010,** *43*, 9608–9612.

23 Kumar, G. S.; Neckers, D. C. *Chem. Rev.* **l989,** *89*, 1915–1925.

24 Shimomura, M.; Kunitake, T. *J. Am. Chem. Soc.* **1987,** *109*, 5175–5183.

25 Tsuda, K.; Dol, G. C.; Gensch T.; Hofkens, J.; Latterini, L.; Weener, J. W.; Meijer, E. W.; Schryver, F. C. D. *J. Am. Chem. Soc.* **2000,** *122*, 3445–3452.

26 Bo, Q.; Zhao, Y. *Langmuir* **2007,** *23*, 5746–5751.

27 Ma, F.; Zhou, N. C.; Zhu, J.; Zhang, W.; Fan, L.; Zhu, X. L. *Eur. Polym. J.* **2009,** *45*, 2131–2137.

28 Han, M.; Hara, M. *J. Am. Chem. Soc.* **2005,** *127*, 10951–10955.

29 Wang, R.; Iyoda, T.; Tryk, D. A.; Hashimoto, K.; Fujishima, A. *Langmuir* **1997,** *13*, 4644–4651.

30 Namiki, K.; Sakamoto, A.; Murata, M.; Kume, S.; Nishihara, H. *Chem. Commun.* **2007,** *44*, 4650–4652.

31 Naito, T.; Horie, K.; Mita, I. *Macromolecules* **1991,** *24*, 2907–2911.

32 Uznanski. P.; Kryszewski, M.; Thulstrup, E. W. *Eur. Polym. J.* **1991,** *27*, 41–43.

33 Parr, R. G.; Weitao, Y. Density Functional Theory of Atoms and Molecules; Oxford University Press: New York, **1989**.